Low-frequency Raman modes and electronic excitations in atomically thin MoS$_2$ films

Hualing Zeng,[1] Bairen Zhu,[1] Kai Liu,[2] Jiahe Fan,[2] Xiaodong Cui,[1,*] and Q. M. Zhang[2,†]

[1]*Department of Physics, The University of Hong Kong, Pokfulam Road, Hong Kong, China*
[2]*Department of Physics, Renmin University of China, Beijing 100872, People's Republic of China*

Atomically thin MoS$_2$ crystals have been recognized as quasi-two-dimensional semiconductors with remarkable physical properties. We report our Raman scattering measurements on multilayer and monolayer MoS$_2$, especially in the low-frequency range (<50 cm^{-1}). We find two low-frequency Raman modes with a contrasting thickness dependence. When increasing the number of MoS$_2$ layers, one mode shows a significant increase in frequency while the other decreases following a $1/N$ (N denotes the number of unit layers) trend. With the aid of first-principles calculations we assign the former as the shear mode E_{2g}^2. The latter is distinguished as the compression vibrational mode, similar to the surface vibration of other epitaxial thin films. The opposite evolution of the two modes with thickness demonstrates vibrational modes in an atomically thin crystal as well as a more precise way to characterize the thickness of atomically thin MoS$_2$ films. In addition, we observe a broad feature around 38 cm^{-1}(5 meV) which is visible only under near-resonance excitation and pinned at a fixed energy, independent of thickness. We interpret the feature as an electronic Raman scattering associated with the spin-orbit coupling induced splitting in a conduction band at K points in their Brillouin zone.

In the hunt for fundamentally thin electronic devices, atomically thin molybdenum disulfide (MoS$_2$) layers have been recognized as a promising material after the success with graphene. A bulk MoS$_2$ crystal has a structure of a S-M-S covalently bonded hexagonal quasi-two-dimensional (2D) network weakly stacked by weak van der Waals forces, as sketched in Fig. 1(a). The MoS$_2$ monolayer, the elementary unit to form ultrathin films by weak stacking, is stable under ambient conditions and is easily fabricated either by mechanical or liquid-phase exfoliation.[1–3] As MoS$_2$ thins to a few atomic layers, there emerge many exotic physical properties absent in bulk crystal. For example, the MoS$_2$ thin film undergoes a transition from an indirect-gap semiconductor with a gap of 1.2 eV in bulk form to a direct-gap one with a band gap of 1.9 eV in monolayers,[4,5] and as well as a possible structural change.[6–8] These distinct physical properties make the atomically thin MoS$_2$ crystal attractive for diverse applications such as electronic devices, spintronics, photovoltaic, energy storage, etc.

Raman scattering has been proven to be valuable as a nondestructive and versatile method of structural characterization and as a method for studying the electronic and vibrational properties in quasi-2D materials. There are four Raman-active vibrational modes in bulk MoS$_2$ crystals, namely, E_{1g} (in-plane optical vibration of S atoms), A_{1g} (out-of-plane optical vibration of S atoms), E_{2g}^1 (in-plane optical vibration of the Mo-S bond), and E_{2g}^2 modes (in-plane optical vibration of the rigid atomic bond).[9] The E_{1g} (in-plane optical vibration of S atoms) of MoS$_2$ thin films is negligible in the backscattering geometry which is widely used in micro-optic spectroscopic studies of nanostructures, owing to the forbidden selection rule from the symmetry point of view. Lee *et al.*[10] investigated the in-plane E_{2g}^1 mode and out-of-plane A_{1g} mode around 400 cm^{-1} in few-layer MoS$_2$ and found that the two modes show an opposite frequency dependence on the film thickness, E_{2g}^1 softening and A_{1g} stiffening with the thickness presumably due to increased dielectric screening, stacking-induced changes in

intralayer bonding, and interlayer coupling. The frequency difference of these two characteristic E_{2g}^1 and A_{1g} modes ranging from 19 cm^{-1} in the monolayer to 26 cm^{-1} in bulk crystal are well accepted as a thickness monitor for atomically thin MoS$_2$ flakes. The E_{2g}^2 mode (in-plane optical vibration of rigidly bonded atoms), also known as the shear mode, originates from the rigid in-plane vibration against adjacent layers and seemingly exists in many layered structures. The energy of the E_{2g}^2 mode is very low,[11] analogously 30–40 cm^{-1} in few-layer graphene,[12] and is hardly observable in many commercial apparatuses due to the limited rejection against Rayleigh scattering.

Here we report our observation of Raman scattering on few-layer MoS$_2$ in the low-frequency range. We find two low-frequency Raman modes (1–6 meV) with contrasting thickness dependence. With an increasing thickness of the MoS$_2$ films, one shows a significant increase in frequency while the other decreases following a $1/N$ (N denotes the number of unit layers) trend. With the aid of first-principles calculations we assign the former as the shear mode E_{2g}^2 and the latter as the compression vibrational mode, similar to the surface vibration of atomically epitaxial thin films. The opposite evolution of the two modes with thickness demonstrates vibrational modes in atomically thin crystals as well as a way to precisely determine the number of MoS$_2$ atomic layers. In addition, we observe a broad feature around 5 meV, which is visible only under near-resonance excitation and locates at a fixed position at various thicknesses.

Ultrathin flakes were mechanically exfoliated from a natural MoS$_2$ single crystal onto silicon wafers capped with 300 nm thick SiO$_2$ by a method analogous to that of producing graphene. Atomically thin MoS$_2$ flakes were first visually screened with interference color through an optical microscope. Typical optical images of MoS$_2$ ultrathin slabs are presented in Fig. 1. The film thickness is confirmed by atomic force microscopy and photoluminescence spectra.[4,5] The Raman scattering is collected through a home-built confocal-like
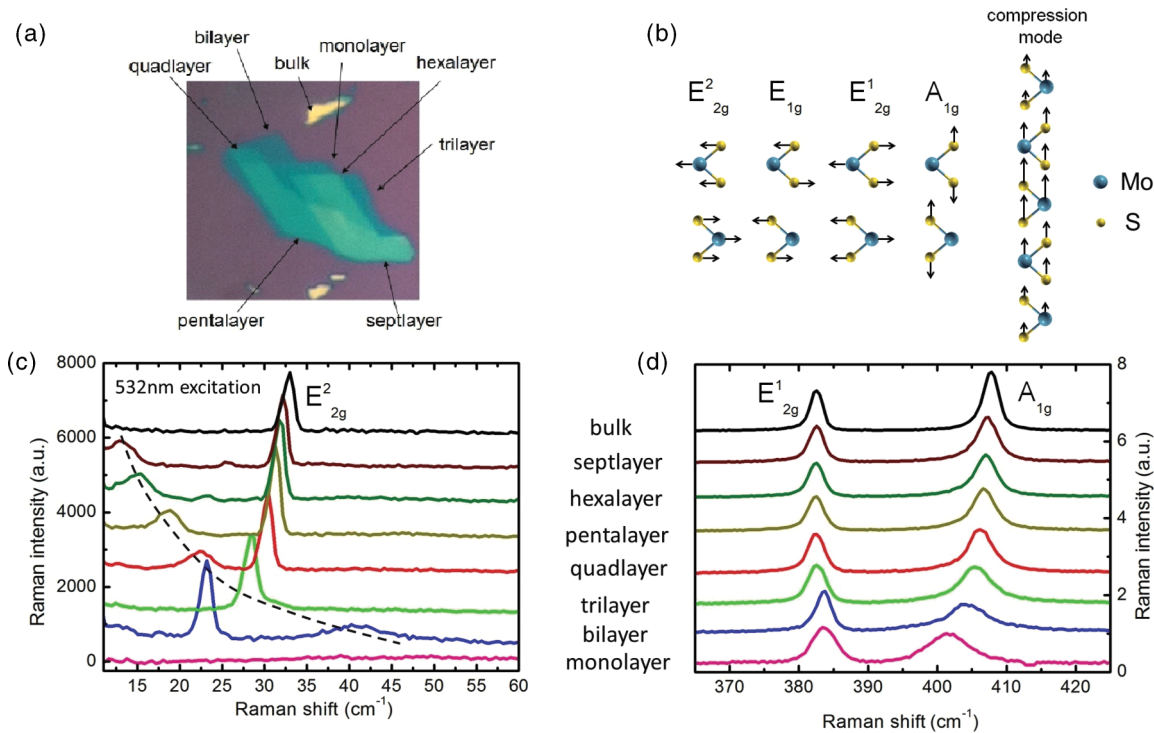
FIG. 1. (Color online) (a) Optical images of ultrathin MoS_2 flakes. (b) Schematics of Raman-active modes. (c) Low-wave-number Raman spectra of atomically thin MoS_2 flakes with different thicknesses under 532 nm excitation. The dashed line denotes the evolution of the weaker low-frequency mode. (d) The corresponding E_{2g}^1 and A_{1g} modes. Their frequency difference is an indicator of the number of layers.

microscopic setup coupled to a triple stage monochromator (Acton TriVista) equipped with a CCD camera under ambient conditions. The laser lines 532 and 633 nm are chosen to be exciting light sources with a beam spot size around 5–10 μm^2 at a power around 300 μW when focused at the samples.

Figure 1 presents the Raman spectra from samples with various thicknesses. The in-plane vibrational E_{2g}^1 mode and the out-of-plane vibrational A_{1g} mode around 400 cm^{-1} show a consistent trend as reported in Ref. 10. The E_{2g}^1 mode stiffens and the A_{1g} mode softens as the sample thins to multilayers and monolayers. The frequency difference between the two modes shows a consistent indication of the layer thickness as other means, particularly for the monolayer, bilayer, trilayer, and quadlayer ($N < 4$). In the low-frequency range, two modes can be clearly seen at various thicknesses except for the monolayer at 532 nm excitation. The mode with a narrow bandwidth (~ 2 cm^{-1}) undergoes a blueshift with increasing thickness, from 22 cm^{-1} in the bilayer to 32 cm^{-1} in bulk form, while the mode with a broad bandwidth undergoes an opposite evolution, as indicated by the dashed line in Fig. 1.

To gain insight into the observed modes, we have studied the zone center phonons of MoS_2 from first-principles density functional theory (DFT) calculations as implemented in the Vienna *ab initio* simulation package.[13–16] The few-layer MoS_2 was modeled as a 1×1 unit cell in two- to five-layer slabs, which were separated by a vacuum > 13 Å in the perpendicular direction. The projector augmented wave (PAW) method[17,18] and the local density approximation (LDA) for exchange-correlation potentials were adopted. The energy cutoff for the plane waves was 400 eV. The first Brillouin zone was sampled with a $12 \times 12 \times 4$ k-point mesh for bulk and a $12 \times 12 \times 1$

mesh for few layers. The Gaussian broadening with a width of 0.05 eV was used for Fermi surface smearing. All ions were fully optimized until the forces were less than 0.01 eV/Å. The vibrational frequencies and displacement patterns of the phonon modes were calculated at the equilibrium structures using the dynamical matrix method, as described in our previous publication.[19] It is worth noting that although the LDA method neglects the van der Waals component of the interaction between the layers, it produces reasonably well the interlayer phonons of MoS_2.[20]

The calculated frequencies of E_{2g}^1 (392.7 cm^{-1}) and A_{1g} (419.3 cm^{-1}) modes at the Brillouin zone center in bulk form show good agreement with our experimental values (382.9 and 408.2 cm^{-1}), as well as with previous experiments[10] (382.0 and 407.5 cm^{-1}) and theoretical results (387.8 and 412.0 cm^{-1}).[20] Here we concentrate on the in-plane shear modes below 50 cm^{-1}, which exhibit a prominent thickness dependence, as shown in Fig. 1. Figure 2 presents the calculated phonon frequencies and displacement patterns for the double-degenerate shear modes (E_{2g}^2 mode) in bulk and few-layer MoS_2. The calculated shear modes, 35.3 cm^{-1} in the bilayer (2L), 37.8 cm^{-1} in the trilayer (3L), 38.8 cm^{-1} in the quadlayer (4L), and 39.0 cm^{-1} in the pentalayer (5L), agree qualitatively well with the corresponding observed sharp peaks around 30 cm^{-1} in Fig. 1. The phonon frequencies of these in-plane shear modes increase from null in the monolayer monotonically with the layer thickness. They show a similar thickness dependence and displacement patterns as the shear modes in multilayer graphene,[12] illustrating their similar origin from the interlayer interactions. So we can safely assign the sharp peaks in Fig. 1 to the shear modes (E_{2g}^2 mode as denoted
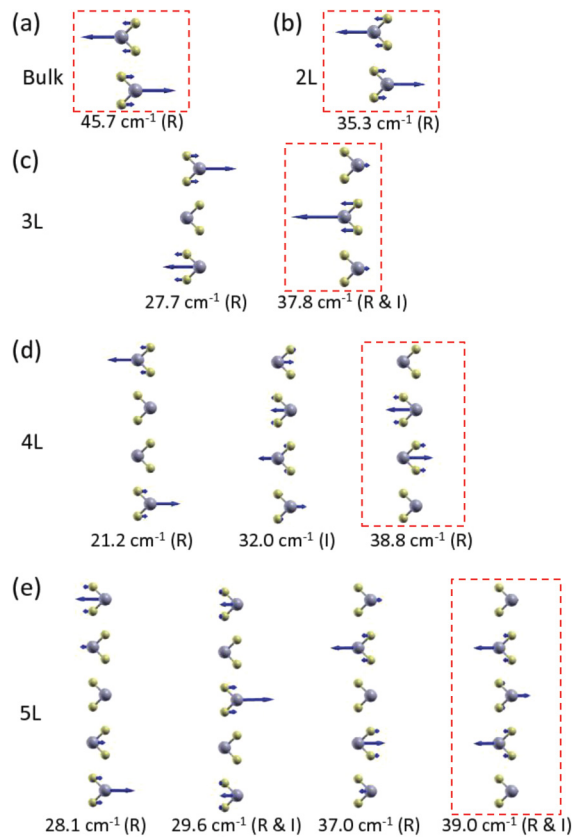
FIG. 2. (Color online) Calculated phonon frequencies and displacement patterns for the shear modes of (a) bulk, (b) bilayer, (c) trilayer, (d) quadlayer, and (e) pentalayer MoS_2 at the Brillouin zone center obtained from DFT calculations. The Raman-active (R) and infrared-active (I) modes are labeled. The atomic structures and displacement patterns were prepared using XCRYSDEN (Ref. 21). The modes for different layers are highlighted with dashed boxes.
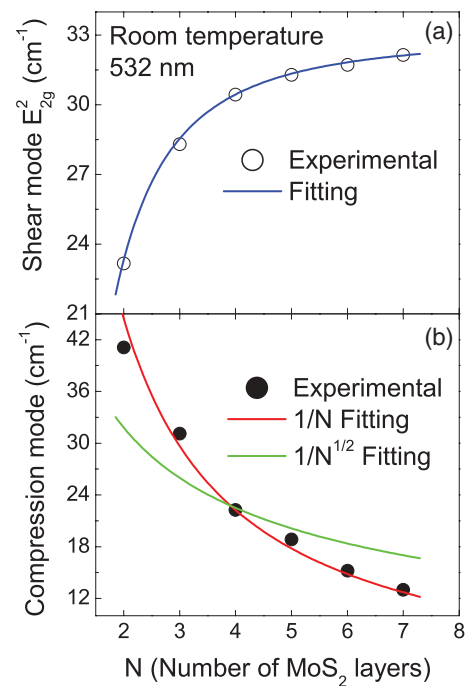

FIG. 3. (Color online) (a) Thickness dependence of frequencies of the E_{2g}^2 shear mode. The blue curve is the fitting with the formula $\omega = \frac{1}{\sqrt{2}\pi c}\sqrt{\frac{\alpha}{\mu}}\sqrt{1 + \cos(\frac{\pi}{N})}$. (b) Thickness dependence of the compression mode (see below) frequencies. The red and green curves are produced with least-squares fitting.

in the bulk) of the adjacent layer oscillation driven by the van der Waals interaction. Our assignments are consistent with previous reports in bulk and few-layer MoS_2.[11,22]

Because such a low-frequency interlayer shear mode is a genuine vibration for layered compounds, we examine the measured peak position of the shear modes with a linear-chain model,[12] $\omega = \frac{1}{\sqrt{2}\pi c}\sqrt{\frac{\alpha}{\mu}}\sqrt{1 + \cos(\frac{\pi}{N})}$, where ω, c, α, μ, and N denote the peak position of the shear mode in cm^{-1}, speed of light in cm/s, the interlayer force constant per unit area, the unit layer mass per unit area, and the number of layers, respectively. Figure 3(a) shows a perfect fitting with the interlayer force constant per unit area $\alpha = 2.9 \times 10^{19}$ N m^{-3} and the single-layer mass per unit area $\mu = 30.3$ kg $Å^{-2}$. One can further estimate the shear modulus $C_{44} = \alpha \times t$ with the spacing t between adjacent MoS_2 layers as $\sim$6.2 Å. This immediately gives $C_{44} \sim 17.9$ GPa. The C_{44} value is in good agreement with the reported experimental shear modulus in MoS_2 bulk crystal, from 15 to 19 GPa.[23,24]

Now we move to the other low-frequency Raman mode. As mentioned above, it cannot be assigned to any known Raman-active mode. It features a contrasting thickness dependence against the E_{2g}^2 mode, as shown in Fig. 3(b). Besides, the thickness dependence follows a perfect $1/N$ rather

than $1/\sqrt{N}$ behavior. The signature of the $1/N$ behavior has been observed in similar thin-film systems with a number of atomic layers grown by molecular beam epitaxy (MBE), such as Na/Cu(001).[25] It is also well understood as an open-ended standing wave mode vertical to atomic planes with a linear-chain force constant model, particularly including the coupling between atomic layers and the substrate.[26] For layered compounds, in principle, there should exist a compression mode besides the shear mode discussed above, which is a rigid-layer vibration vertical to atomic planes. The longitudinal-like open standing wave will give an effective relative shift between adjacent layers if one looks at its vibration amplitude, as shown in Fig. 1(b). That means it actually corresponds to the compression mode. The compression mode, in combination with a longitudinal optical phonon mode, has been experimentally revealed in few-layer graphene through double-resonant intravalley scattering.[27] The mode strongly depends on the coupling between atomic layers and substrate, and the Raman intensity of the mode is much smaller than that of the shear mode. This may be the reason why it is not easily observed in few-layer graphene and MoS_2.

The direct observation of the shear mode and the compression mode provides a way to more precisely characterize the thickness of ultrathin MoS_2. A conventional method is to measure the frequency difference between the A_{1g} and E_{2g}^1 modes. Considering the contrasting evolution of the two rigid-layer low-frequency modes with thickness and the large relative shift up to 100%, the frequency difference between the shear mode and the compression mode would be a more
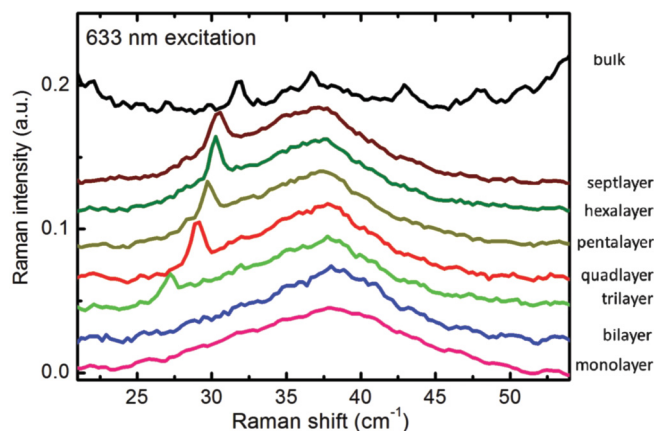
FIG. 4. (Color online) Low-wave-number Raman spectra of MoS_2 thin films at different thicknesses under near-resonant excitation (633 nm). The broad feature around 38 cm^{-1} is observed only in near-resonant excitation.

precise measure of the layer number, particularly for slabs with more than three unit layers.

Another finding in our Raman measurements is the broad feature centered at 38 cm^{-1} (∼5 meV) measured with both cross and parallel polarization configurations under near-resonant excitation. Here, we present the spectrum measured in the cross polarization geometry, which shows clearer features due to the suppressed Rayleigh scattering of the exciting laser line, as shown in Fig. 4. The feature does not change in either position or shape with thickness. We can exclude first-order or higher-order phonons as their origins. Moreover, it is visible only at near-resonance excitation (∼1.96 eV), which is very close to the direct band gap at K points in the Brillouin zone. This implies that the feature might be related to a vertical electronic transition crossing direct band gap.

First the exciton mechanism could be excluded due to the energy scale difference. The so-called A and B excitons in bulk MoS_2 are characterized with binding energies of ∼42 and 134 meV,[28] and recent optical experiments indicated that the two excitonic states exhibit little change in few-layer MoS_2 compared to bulk materials.[4,5] The exciton binding energies are much larger than that of the broad feature around 5 meV. Impurity or defect states are also unlikely to contribute to this feature from the energy scale. Impurity and defects states appearing in optical measurements are of the same energy

scale as the exciton binding energy.[5] It should be noted that our samples and those used in the optical measurements are from the same source (SPI Supplies). Similar conditions of the impurities and defects could be expected in our samples if they existed. Collective electric carrier oscillation, the so-called plasmon mode, and other collective modes such as the charge density wave (CDW) are also excluded from the fact of thickness independence, as Coulomb screening and interlayer coupling would be strongly dependent on thickness.

The potential mechanism responsible for the broad feature may lie in the spin-orbit coupling in the conduction band at K points in their Brillouin zone. Recent band structure calculations[29,30] indicated that spin-orbit coupling contributes to the splitting at the top of valence band at K points ($v1$ and $v2$), which are the origins of A and B excitons. At the same time, spin-orbit coupling also induces a subtle splitting of ∼4 meV at the conduction band at K points. The subtle splitting would be reflected in a resonantlike Raman procedure crossing the direct band gap at K points. This naturally explains why it appears only at near-resonant excitations. The thickness-independent Raman feature manifests the thickness-independent spin-orbit coupling induced splitting in the conduction band.

In conclusion, two low-frequency modes, the shear mode and the compression mode, are investigated in present Raman measurements. They exhibit a completely opposite evolution with the thickness of ultrathin MoS_2. The pair of low-frequency modes provides a more precise method to characterize the thickness of an atomically thin MoS_2 crystal. We also observe a broad feature at ∼5 meV which is likely related to the electronic structure. We point out that the feature may originate from the spin-orbit coupling induced splitting at the conduction band at K points in their Brillouin zone.

*xdcui@hku.hk

†qmzhang@ruc.edu.cn

[1]P. Joensen, R. F. Frindt, and S. R. Morrison, Mater. Res. Bull. **21**, 457 (1986).

[2]K. S. Novoselov, D. Jiang, F. Schedin, T. J. Booth, V. V. Khotkevich, S. V. Morozov, and A. K. Geim, Proc. Natl. Acad. Sci. USA **102**, 10451 (2005).

[3]J. N. Coleman *et al.*, Science **331**, 568 (2011).

[4]K. F. Mak, C. Lee, J. Hone, J. Shan, and T. F. Heinz, Phys. Rev. Lett. **105**, 136805 (2010).

[5]A. Splendiani, L. Sun, Y. Zhang, T. Li, J. Kim, C.-Y. Chim, G. Galli, and F. Wang, Nano Lett. **10**, 1271 (2010).

[6]D. Yang, S. J. Sandoval, W. M. R. Divigalpitiya, J. C. Irwin, and R. F. Frindt, Phys. Rev. B **43**, 12053 (1991).

[7]S. Jiménez Sandoval, D. Yang, R. F. Frindt, and J. C. Irwin, Phys. Rev. B **44**, 3955 (1991).

[8]X. R. Qin, D. Yang, R. F. Frindt, and J. C. Irwin, Phys. Rev. B **44**, 3490 (1991).

[9]J. L. Verble and T. J. Wieting, Phys. Rev. Lett. **25**, 362 (1970).

[10]C. Lee, H. Yan, L. E. Brus, T. F. Heonz, J. Hone, and S. Ryu, ACS Nano **4**, 2695 (2010).

[11]G. Plechinger, S. Heydrich, J. Eroms, D. Weiss, C. Schüller, and T. Korn, Appl. Phys. Lett. **101**, 101906 (2012).

[12] P. H. Tan, W. P. Han, W. J. Zhao, Z. H. Wu, K. Chang, H. Wang, Y. F. Wang, N. Bonini, N. Marzari, N. Pugno, G. Savini, A. Lombardo, and A. C. Ferrari, Nat. Mater. **11**, 294 (2012).

[13] G. Kresse and J. Hafner, Phys. Rev. B **47**, 558 (1993).

[14] G. Kresse and J. Hafner, Phys. Rev. B **49**, 14251 (1994).

[15] G. Kresse and J. Furthmüller, Phys. Rev. B **54**, 11169 (1996).

[16] G. Kresse and J. Furthmüller, Comput. Mater. Sci. **6**, 15 (1996).

[17] P. E. Blöchl, Phys. Rev. B **50**, 17953 (1994).

[18] G. Kresse and D. Joubert, Phys. Rev. B **59**, 1758 (1999).

[19] A. M. Zhang, K. Liu, J. H. Xiao, J. B. He, D. M. Wang, G. F. Chen, B. Normand, and Q. M. Zhang, Phys. Rev. B **85**, 024518 (2012).

[20] A. Molina-Sánchez and L. Wirtz, Phys. Rev. B **84**, 155413 (2011).

[21] A. Kokalj, Comput. Mater. Sci. **28**, 155 (2003).

[22] J. L. Verble, T. J. Wietling, and P. R. Reed, Solid State Commun. **11**, 941 (1972).

[23] J. L. Feldman, J. Phys. Chem. Solids **37**, 1141 (1976).

[24] *Mechanics of Coatings: Proceedings of the 16th Leeds-Lyon Symposium on Tribology*, Institute National Des Sciences Appliquées, Lyon, France, 5–8 September 1989, edited by D. Dowson, C. M. Taylor, and M. Godet (Elsevier, Amsterdam, 1990).

[25] G. Benedek, J. Ellis, A. Reichmuth, P. Ruggerone, H. Schief, and J. P. Toennies, Phys. Rev. Lett. **69**, 2951 (1992).

[26] N. S. Luo, P. Ruggerone, and J. P. Toennies, Phys. Rev. B **54**, 5051 (1996).

[27] F. Herziger, P. May, and J. Maultzsch, Phys. Rev. B **85**, 235447 (2012).

[28] R. Coehoorn, C. Haas, and R. A. de Groot, Phys. Rev. B **35**, 6203 (1987).

[29] T. Cheiwchanchamnangij and W. R. L. Lambrecht, Phys. Rev. B **85**, 205302 (2012).

[30] D. Xiao, G.-B. Liu, W. Feng, X. Xu, and W. Yao, Phys. Rev. Lett. **108**, 196802 (2012).